

Experimental determination of the evolution of the Bjorken integral at low Q^2

A. Deur¹, P. Bosted^{1,2}, V. Burkert¹, G. Cates³, J.-P. Chen¹, Seonho Choi⁴, D. Crabb³, C.W. de Jager¹, R. De Vita⁵, G. E. Dodge⁶, R. Fatemi³, T. A. Forest⁷, F. Garibaldi⁸, R. Gilman^{1,9}, E. W. Hughes¹⁰, X. Jiang⁹, W. Korsch¹¹, S. E. Kuhn⁶, W. Melnitchouk¹, Z.-E. Meziani⁴, R. Minehart³, A. V. Skabelin¹², K. Slifer^{3,4}, M. Taiuti⁵, J. Yun⁶

¹Thomas Jefferson National Accelerator Facility, Newport News, VA 23606

²University of Massachusetts, Amherst MA 01002

³University of Virginia, Charlottesville, VA 22904

⁴Temple University, Philadelphia, PA 19122

⁵INFN, Sezione di Genova, 16146 Genova, Italy

⁶Old Dominion University, Norfolk, VA 23529

⁷Louisiana Tech University, Ruston, LA 71272

⁸ISS/INFN Roma1, gr. coll. Sanita', Viale Regina Elena 299, 00161 Rome, Italy

⁹Rutgers University, Piscataway, NJ 08854

¹⁰California Institute of Technology, Pasadena, CA 91125

¹¹University of Kentucky, Lexington, KY 40506

¹²Massachusetts Institute of Technology, Cambridge, MA 02139

(Dated: July 18, 2018)

We extract the Bjorken integral Γ_1^{p-n} in the range $0.17 < Q^2 < 1.10 \text{ GeV}^2$ from inclusive scattering of polarized electrons by polarized protons, deuterons and ^3He , for the region in which the integral is dominated by nucleon resonances. These data bridge the domains of the hadronic and partonic descriptions of the nucleon. In combination with earlier measurements at higher Q^2 , we extract the non-singlet twist-4 matrix element f_2 .

PACS numbers: 13.60.Hb, 11.55.Hx, 25.30.Rw, 12.38.Qk, 24.70.+s

For almost 50 years experimental and theoretical research efforts in hadronic physics have sought to understand the structure of the nucleon. With the development of Quantum Chromodynamics (QCD), these studies have focused on obtaining an accurate description of nucleon structure in terms of fundamental quark and gluon degrees of freedom. A powerful tool has been deep inelastic lepton scattering from nucleons and nuclei, and the associated theoretical machinery of the operator product expansion (OPE), which allows the interpretation of the measured structure functions in terms of parton momentum and spin distribution functions.

Experiments using polarized beams and targets have played a critical role in testing the application of QCD to nucleon structure [1]. The Bjorken sum rule [2], which relates the first moment of polarized deep inelastic structure functions to nucleon ground state properties, has been an important part of these studies. At infinite four-momentum transfer squared, Q^2 , the sum rule reads

$$\Gamma_1^{p-n} \equiv \Gamma_1^p - \Gamma_1^n \equiv \int_0^1 dx (g_1^p(x) - g_1^n(x)) = \frac{g_A}{6}, \quad (1)$$

where g_1^p and g_1^n are the spin-dependent proton and neutron structure functions, respectively. Here, g_A is the nucleon axial charge and $x = Q^2/2M\nu$, with ν the energy transfer and M the nucleon mass. The sum rule has been verified experimentally to better than 10% [3, 4, 5].

Because the Bjorken sum rule relates differences of proton and neutron structure function moments, Γ_1^p and Γ_1^n , only flavor non-singlet quark operators appear in the OPE. Another simplification arises at low Q^2 where the

resonance contributions to the proton and neutron, in particular that of the $\Delta(1232)$ resonance, partly cancel. This cancellation simplifies calculations based on chiral perturbation theory (χ PT), and may extend the Q^2 range of their applicability. The gap between the domains of validity for perturbative QCD (pQCD) and χ PT might even be bridged, enabling for the first time a fundamental theoretical description of nucleon structure from large to small scales [6]. The Bjorken sum rule is therefore relevant for understanding the transition from pQCD to nonperturbative QCD.

In this Letter we report on a determination of the Bjorken integral using data obtained at the Thomas Jefferson National Accelerator Facility (Jefferson Lab) over the Q^2 range of 0.17–1.10 GeV^2 . Combined with higher Q^2 data from earlier experiments, we analyze the data using the OPE and extract the $1/Q^2$ higher twist corrections to the integral at intermediate values of Q^2 .

The data were obtained in three different experiments using polarized electrons on polarized proton [7], deuterium [8] and ^3He [9, 10] targets. To analyze the scattered electrons, the proton and deuteron experiments used the CEBAF Large Acceptance Spectrometer (CLAS) in Hall B [11], while the ^3He experiment used the two High Resolution Spectrometers in Hall A [12].

The individual measurements of the proton, neutron and deuteron integrals $\Gamma_1^{p,n,d}$ have been reported elsewhere [7, 8, 9, 10]. To form the isovector combination Γ_1^{p-n} we subtract from the experimental values of g_1^p the values of g_1^n extracted from the ^3He or the deuteron measurements. However, in order to combine these data, the

TABLE I: Inelastic contributions to the Bjorken sum. The second and third columns give the sum and its uncertainty for $W < 2$ GeV. The fourth to sixth columns give the total sum and its uncertainties. The last column indicates the origin of the neutron information (from ^3He or from deuteron data).

Q^2 (GeV 2)	$\Gamma_{1(res)}^{p-n}$	$\sigma_{(res)}^{syst}$	$\Gamma_{1(Tot)}^{p-n}$	$\sigma_{(Tot)}^{syst}$	σ^{stat}	n
0.17	0.0134	0.0073	0.0326	0.0076	0.0057	^3He
0.30	0.0181	0.0079	0.0510	0.0085	0.0039	^3He
0.34	0.0498	0.0165	0.0864	0.0202	0.0266	D
0.47	0.0381	0.0071	0.0860	0.0089	0.0025	^3He
0.53	0.0507	0.0121	0.1035	0.0170	0.0095	D
0.66	0.0394	0.0058	0.1019	0.0095	0.0020	^3He
0.79	0.0395	0.0122	0.1107	0.0176	0.0076	D
0.81	0.0413	0.0056	0.1138	0.0109	0.0019	^3He
0.99	0.0400	0.0049	0.1229	0.0120	0.0019	^3He
1.10	0.0477	0.0084	0.1366	0.0166	0.0076	D

Q^2 values at which g_1^p and g_1^n were obtained must coincide. We chose to re-analyze the ^3He data at six values of Q^2 which match the ones of the proton data and differ from the values reported in Refs. [9, 10]. For the deuteron measurement, given the larger uncertainties, we simply interpolated the proton data points to match the four Q^2 points of the deuteron data. The additional systematic uncertainty from the interpolation is negligible.

The three experiments [7, 8, 9, 10] have measured g_1 up to an invariant mass $W = 2$ GeV. The unmeasured contributions to the proton and neutron integrals, corresponding to the low- x domain, need to be consistently accounted for. In the current analysis, the fit from Bianchi and Thomas [13] was used to estimate the low- x contribution to the moments up to $W^2 = 1000$ GeV 2 . The uncertainty on this contribution was evaluated by taking the quadratic sum of the differences induced by independently varying each parameter of the fit within the range of values given in [13]. The contribution beyond 1000 GeV 2 was determined using a Regge parametrization constrained so that the Bjorken integral at $Q^2 = 5$ GeV 2 , from the world data complemented by the Bianchi and Thomas fit and our Regge parametrization, agrees with the sum rule. The systematic uncertainties from the neutron and proton data have been added in quadrature. The moment Γ_1^n was extracted from ^3He or deuterium data using the formalism of nucleon effective polarizations [14, 15]. The resulting Γ_1^{p-n} is shown in Fig. 1 by the filled symbols, with the values given in Table I. Note that only the inelastic contributions are included in Γ_1^{p-n} . Data from the SLAC E143 experiment [16] are also shown (open circles) for comparison.

The data are compared with theoretical calculations based on χPT and with phenomenological models. At $Q^2 = 0$, the slope of the Bjorken integral is constrained by the Gerasimov-Drell-Hearn (GDH) sum rule [17, 18]. The Soffer-Teryaev model [19] agrees only with the low- Q^2 data. The overestimate at larger Q^2 was traced back

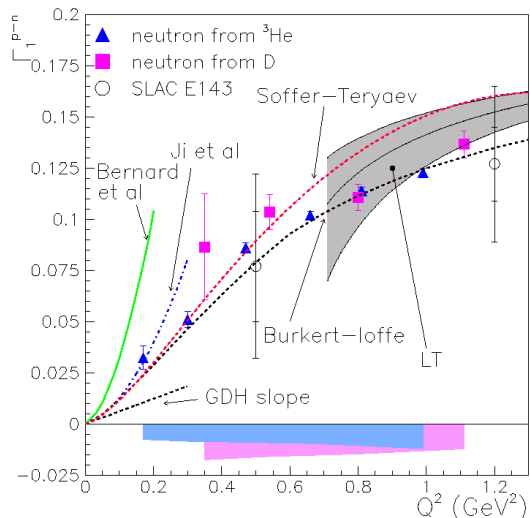


FIG. 1: Inelastic contribution to the Bjorken sum. The triangles (squares) represent the results with the neutron extracted from ^3He (deuteron) data, with the horizontal bands covering the 0.17-0.99 GeV 2 and 0.34-1.1 GeV 2 ranges the corresponding systematic uncertainties. The E143 data are shown for comparison. The gray band represents the leading-twist (LT) contribution calculated to third order in α_s . The curves correspond to theoretical calculations (see text).

to the QCD radiative corrections and has now been corrected [20]. The Burkert-Ioffe model [21] agrees well with the data over the full range covered in Fig. 1. This may indicate that vector meson dominance gives a reasonable picture of the parton-hadron transition. At low Q^2 attempts have also been made to calculate Γ_1^{p-n} using χPT [22, 23]. The calculation done in the heavy baryon approximation [23] seems to agree better with the data. At higher Q^2 the data are compared with the leading-twist calculation (gray band in Fig. 1), which corresponds to incoherent scattering from individual quarks. In pQCD, gluon radiation causes scaling violations in structure functions, and introduces an α_s dependence on the right hand side of Eq. (1). At leading-twist, the pQCD result at third order in α_s (in the $\overline{\text{MS}}$ scheme) is

$$\Gamma_1^{p-n} = \frac{g_A}{6} \left[1 - \frac{\alpha_s}{\pi} - 3.58 \left(\frac{\alpha_s}{\pi} \right)^2 - 20.21 \left(\frac{\alpha_s}{\pi} \right)^3 \right]. \quad (2)$$

The gray band in Fig. 1 represents the uncertainty in Γ_1^{p-n} due to the uncertainty in α_s . There is reasonable agreement between the leading-twist prediction and the data. Their difference is related to higher twist effects that should become important at low Q^2 . In particular, application of the OPE to moments of structure functions requires the expansion of the *total* moment rather than the *inelastic* moment as in Fig. 1. While the elastic contribution is negligible at high Q^2 , it dominates at low

Q^2 . Fig. 2 shows the total moment, including the elastic contribution, calculated from the form factor parameterizations from Ref. [24]. In addition to the JLab data, we also plot data at higher Q^2 from the SLAC E143 [25] and E155 [4], DESY HERMES [26] and CERN SMC [5] experiments. For consistency, the low- x contributions, outside of the measured regions, have been re-evaluated using the same procedure as described earlier.

The OPE analysis allows one to expand the total moment Γ_1^{p-n} in powers of $1/Q^2$:

$$\Gamma_1^{p-n} = \sum_{i=1}^{\infty} \frac{\mu_{2i}^{p-n}}{Q^{2i-2}}, \quad (3)$$

where the leading twist $i = 1$ coefficient is given in Eq. (2). The coefficients μ_{2i}^{p-n} for $i > 1$ represent matrix elements of higher twist operators. The matrix elements contain information on the long range, nonperturbative interactions or correlations between partons. In particular, the $1/Q^2$ correction term is [27, 28]

$$\mu_4^{p-n} = \frac{M^2}{9} (a_2^{p-n} + 4d_2^{p-n} + 4f_2^{p-n}), \quad (4)$$

where a_2^{p-n} is the target mass correction given by the x^2 -weighted moment of the leading-twist g_1 structure function, and d_2^{p-n} is a twist-3 matrix element given by

$$d_2^{p-n} = \int_0^1 dx x^2 (2g_1^{p-n} + 3g_2^{p-n}). \quad (5)$$

The twist-4 contribution, f_2^{p-n} , given by a mixed quark-gluon operator, is related to the color electric and magnetic polarizabilities of the nucleon [29, 30].

The a_2^{p-n} correction, which is twist-2, is calculated using the fit of polarized parton distributions from Ref. [31]. The d_2^{p-n} matrix element is obtained from [32]. With these inputs, the data on Γ_1^{p-n} in Fig. 2 can be used to extract f_2^{p-n} . As an additional parameter in the fit, we include the $1/Q^4$ coefficient μ_6^{p-n} . For the leading twist contribution, we constrain the low- x extrapolation by assuming the validity of the Bjorken sum rule for $Q^2 > 5 \text{ GeV}^2$. In fact, our low- x extrapolation gives $g_A^{\text{fit}} = 1.270 \pm 0.045$, which is very close to the empirical value $g_A = 1.267 \pm 0.004$. The higher twist terms are then determined from the $Q^2 < 5 \text{ GeV}^2$ data using our fitted value of g_A . The point to point correlated uncertainty for the JLab data extracted from ^3He and hydrogen has been disentangled from the uncorrelated uncertainty, and only the latter is used in the fit. The correlated systematics are then propagated to the fit result, as is the uncertainty arising from α_s . The data from the other experiments are treated as uncorrelated from point to point.

It is not clear *a priori* over which Q^2 range the $1/Q^2$ expansion should be valid. For instance, at $Q^2 \approx 0.7 \text{ GeV}^2$ the elastic and leading twist contributions are of comparable magnitude. Fitting over the range $0.8 < Q^2 <$

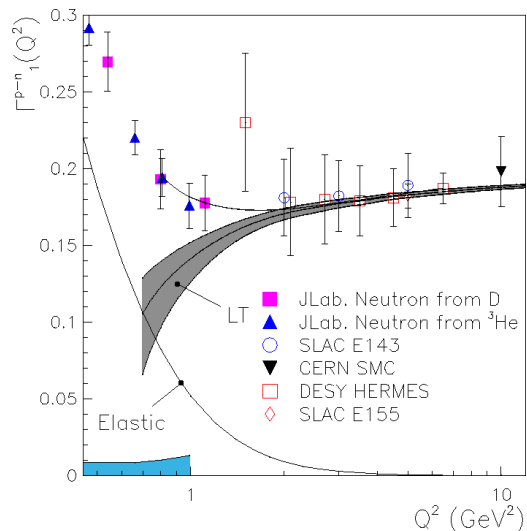


FIG. 2: Total moment Γ_1^{p-n} , including the inelastic contribution from Fig. 1 together with the elastic. The data extracted from ^3He (deuterium) together with proton data are indicated by the triangles (squares). The leading-twist (LT) contribution is given by the gray band. The point to point correlated uncertainty for the data extracted from ^3He and proton is shown by the horizontal band. The error bars on the symbols represent the uncorrelated uncertainty. The data from other experiments are assumed to be uncorrelated. The fits to the total moment are indicated by the solid curves.

10 GeV^2 gives $f_2^{p-n} = -0.13 \pm 0.15(\text{uncor})_{-0.03}^{+0.04}(\text{cor})$, normalized at $Q^2 = 1 \text{ GeV}^2$, where the first and second errors are uncorrelated and correlated, respectively, and $\mu_6^{p-n}/M^4 = 0.09 \pm 0.06(\text{uncor}) \pm 0.01(\text{cor})$. The contribution to the total uncertainty from the elastic form factors is negligible. Starting the fit at a lower Q^2 , $Q^2 = 0.66 \text{ GeV}^2$, yields the more negative value $f_2^{p-n} = -0.18 \pm 0.05(\text{uncor})_{-0.05}^{+0.04}(\text{cor})$, and a larger value for μ_6^{p-n} , $\mu_6^{p-n}/M^4 = 0.12 \pm 0.02(\text{uncor}) \pm 0.01(\text{cor})$, with somewhat smaller errors. The results of the two fits are shown in Fig. 2, but are almost indistinguishable. At $Q^2 = 1 \text{ GeV}^2$, the $1/Q^4$ contribution is $\mu_6^{p-n}/Q^4 \simeq 0.09 \pm 0.02$, which is of similar magnitude and of opposite sign to the $1/Q^2$ term, $\mu_4^{p-n}/Q^2 \simeq -0.06 \pm 0.02$, obtained by adding the extracted f_2^{p-n} value to d_2^{p-n} and a_2^{p-n} in Eq. (4). This may explain why the leading twist description agrees well with the data down to surprisingly small values of Q^2 ($\sim 1 \text{ GeV}^2$), and could be a hint that quark-hadron duality might work well for $p-n$ non-singlet quantities.

These results also suggest that at these lower Q^2 values the twist expansion may not converge very quickly, and that higher twist terms may be needed. Including a μ_8^{p-n}/Q^6 term, however, gives significantly larger uncertainties on the higher twist contributions, making them compatible with zero. Starting the fit at $Q^2 = 0.47 \text{ GeV}^2$,

for instance, gives $f_2^{p-n} = -0.14 \pm 0.10(\text{uncor}) \pm 0.04(\text{cor})$, $\mu_6^{p-n}/M^4 = 0.09 \pm 0.08(\text{uncor})_{-0.04}^{+0.03}(\text{cor})$ and $\mu_8^{p-n}/M^6 = 0.01 \pm 0.03(\text{uncor}) \pm 0.02(\text{cor})$.

The results for f_2^{p-n} can be compared to non-perturbative model predictions: $f_2^{p-n} = -0.024 \pm 0.012$ [29] and $f_2^{p-n} = -0.032 \pm 0.051$ [33] (QCD sum rules), $f_2^{p-n} = 0.028$ [34] (MIT bag model) and $f_2^{p-n} = -0.081$ [35] (instanton model). The results can also be compared with values obtained in analyses of the proton [36] and neutron [37] data separately. Naively subtracting f_2^n from f_2^p gives 0.01 ± 0.08 , which is consistent within uncertainties with the above values for f_2^{p-n} . However, different Q^2 ranges were used in the proton and neutron fits, and different low- x extrapolations implemented.

The larger uncertainty on f_2^{p-n} from the $Q^2 > 0.8 \text{ GeV}^2$ analysis reflects the larger values of Q_{min}^2 used here compared with that used in the neutron analysis [37]. Fitting the neutron data from $Q^2 = 1 \text{ GeV}^2$ rather from $Q^2 = 0.5 \text{ GeV}^2$ as in Ref. [37] would increase the uncertainty on f_2^n appreciably, which, when combined with the proton data fitted over the same range, would be more compatible with the uncertainty from the present combined analysis. This issue could be ameliorated with better quality data at higher Q^2 ($Q^2 > 1 \text{ GeV}^2$). Data in this region on the proton and deuteron collected in Hall B at Jefferson Lab are presently being analysed. Plans for high-precision measurements of the proton and neutron structure functions at higher Q^2 are also included in the 12 GeV energy upgrade of Jefferson Lab [38].

To summarize, we have presented an extraction of the Bjorken sum in the $0.17 < Q^2 < 1.10 \text{ GeV}^2$ range. Being a nonsinglet quantity, the Bjorken sum simplifies the theoretical analyses at both high Q^2 (using the OPE) and at low Q^2 (using χ PT). It thus provides us with a unique opportunity to understand better the transition from perturbative QCD to the confinement region. Combining with data at higher Q^2 , we have extracted the higher twist contributions to the sum. We find f_2^{p-n} small and the total higher twist contribution, for twists lower than eight, compatible with zero.

This work was supported by the U.S. Department of Energy (DOE) and the U.S. National Science Foundation. The Southeastern Universities Research Association operates the Thomas Jefferson National Accelerator Facility for the DOE under contract DE-AC05-84ER40150.

[1] See for example B. W. Filippone and X. Ji, *Adv. Nucl. Phys.* **26**, 1 (2001) and references therein.
 [2] J. D. Bjorken, *Phys. Rev.* **148**, 1467 (1966).
 [3] E154 collaboration: K. Abe *et al.*, *Phys. Rev. Lett.* **79**, 26 (1997).

[4] E155 collaboration: P. L. Anthony *et al.*, *Phys. Lett.* **B493**, 19 (2000).
 [5] SMC collaboration: D. Adeva *et al.*, *Phys. Rev. D* **58**, 112001 (1998).
 [6] V. D. Burkert, *Phys. Rev. D* **63**, 097904 (2001).
 [7] CLAS collaboration: R. Fatemi *et al.*, *Phys. Rev. Lett.* **91**, 222002 (2003).
 [8] CLAS collaboration: J. Yun *et al.*, *Phys. Rev. C* **67**, 055204 (2003).
 [9] E94-010 collaboration: M. Amarian *et al.*, *Phys. Rev. Lett.* **89**, 242301 (2002).
 [10] E94-010 collaboration: M. Amarian *et al.*, *Phys. Rev. Lett.* **92**, 022301 (2004).
 [11] CLAS collaboration: B. A. Mecking *et al.*, *Nucl. Inst. Meth.* **A503**, 513 (2003).
 [12] Hall A collaboration: J. Alcorn *et al.*, *Nucl. Inst. Meth.* **A522**, 294 (2004).
 [13] N. Bianchi and E. Thomas, *Nucl. Phys. Proc. Suppl.* **82**, 256 (2000).
 [14] See e.g. C. Ciofi degli Atti and S. Scopetta, *Phys. Lett.* **B404**, 223 (1997).
 [15] M. Lacombe *et al.*, *Phys. Rev. C* **21**, 861 (1980)
 [16] E143 collaboration: K. Abe *et al.*, *Phys. Rev. Lett.* **78**, 815 (1997).
 [17] S. D. Drell and A. C. Hearn, *Phys. Rev. Lett.* **16**, 908 (1966). S. Gerasimov, *Sov. J. Nucl. Phys.* **2**, 430 (1966).
 [18] X. Ji and J. Osborne, *J.Phys. G* **27** 127 (2001).
 [19] J. Soffer and O. V. Teryaev, *Phys. Lett.* **B545**, 323 (2002).
 [20] J. Soffer, hep-ph/0409333.
 [21] V. D. Burkert and B. L. Ioffe, *Phys. Lett.* **B296**, 223 (1992); *J. Exp. Theor. Phys.* **78**, 619 (1994).
 [22] V. Bernard, T. R. Hemmert and Ulf-G. Meißner, *Phys. Rev. D* **67**, 076008 (2003).
 [23] X. Ji, C. W. Kao and J. Osborne, *Phys. Lett.* **B472**, 1 (2000).
 [24] P. Mergell, U.-G. Meißner and D. Drechsel, *Nucl. Phys.* **A596**, 367 (1996).
 [25] E143 collaboration: K. Abe *et al.*, *Phys. Rev. D* **58**, 112003 (1998).
 [26] HERMES collaboration: A. Airapetian *et al.*, *Eur. Phys. J. C* **26**, 527 (2003).
 [27] E. V. Shuryak and A. I. Vainshtein, *Nucl. Phys.* **B201**, 141 (1982).
 [28] X. Ji and P. Unrau, *Phys. Lett.* **B333**, 228 (1994).
 [29] E. Stein *et al.*, *Phys. Lett.* **B353**, 107 (1995).
 [30] X. Ji, *Baryons '95: Proceedings of the 7th International Conference on the Structure of Baryons*, Santa Fe, New Mexico, B. F. Gibson, P. D. Barnes, J. B. McClelland, and W. Weise ed. (World Scientific, New Jersey, 1996).
 [31] J. Bluemlein and H. Boettcher, *Nucl. Phys.* **B636**, 225 (2002).
 [32] Jefferson Lab Hall A collaboration: X. Zheng *et al.*, nucl-ex/0405006, submitted to *Phys. Rev. C*.
 [33] I.I. Balitsky, V.M. Braun, A.V. Kolesnichenko, *Phys. Lett.* **B242**, 245 (1990); *Erratum-ibid* **B318**, 648 (1993).
 [34] X. Ji, Rep. No. MIT-CTP-2468 (1995); hep-ph/9509288.
 [35] N.Y. Lee, K. Goeke and C. Weiss, *Phys. Rev. D* **65**, 054008 (2002).
 [36] M. Osipenko *et al.*, hep-ph/0404195.
 [37] E94-010 collaboration: Z. E. Meziani *et al.*, hep-ph/0404066.
 [38] *The Science Driving the 12 GeV Upgrade at CEBAF*, http://www.jlab.org/div_dept/physics_division/GeV.html.